

# Ideal MHD equilibria of tokamak plasmas

by J. Blasco, P. Díez, M. Pellicer, and A. Rodríguez-Ferran

## 6.1 Introduction

A tokamak is a device that confines a plasma by means of a toroidal magnetic field (see <http://en.wikipedia.org/wiki/Tokamak>). The ultimate goal is the generation of energy through nuclear fusion. Several experimental tokamaks are currently in operation. A world-wide consortium (including, among others, the European Union, USA, Russia, Japan, and China) has launched the ITER initiative (Figure 6.1), “aimed at demonstrating that this energy source [fusion] can be used to produce electricity in a safe and environmentally benign way, with abundant fuel resources, to meet the needs of a growing world population” (see <http://www.iter.org>).

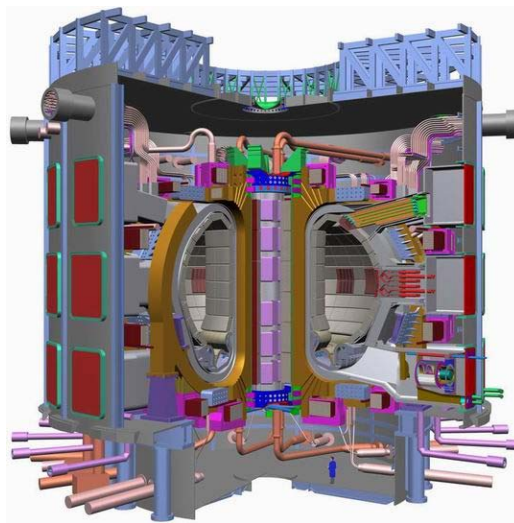


Figure 6.1: The ITER device (from <http://www.iter.org>).

In a tokamak, the confining magnetic field is generated by means of external coils (the term “tokamak”, of Russian origin, stands for “toroidal chamber with magnetic coils”). For stable equilibria, azimuthal (i.e., rotational) symmetry is required.

### 6.1.1 General problem

A well established result in the field of magnetohydrodynamics (MHD) is that plasma equilibrium under such axi-symmetric conditions can be modelled by means of the so-called Grad–Shafranov equation (see, for instance, [2] and the references therein), which reads

$$L\Psi = j \quad \text{with} \quad j = \begin{cases} j(\Psi) & \text{in } \Omega_P \\ j_C & \text{in } \Omega_C \\ 0 & \text{in } \Omega_V \cup \Omega_A \end{cases} \quad (6.18)$$

In Equation (6.18),  $\Psi$  is the flux function,  $L$  is the 2D Laplacian-type operator in cylindrical coordinates,

$$L\Psi = -\frac{\partial}{\partial r} \left( \frac{1}{\mu_0 r} \frac{\partial \Psi}{\partial r} \right) - \frac{\partial}{\partial z} \left( \frac{1}{\mu_0 r} \frac{\partial \Psi}{\partial z} \right),$$

with  $\mu_0$  the magnetic permeability, and  $j$  is the electric current, which depends on the flux function in the plasma  $\Omega_P$ , is constant in the coils  $\Omega_C$  and is zero in  $\Omega_V$  (void inside the chamber) and  $\Omega_A$  (outer domain); see Figure 6.2. This partial differential equation is complemented with appropriate boundary conditions.

The Grad–Shafranov equation is nonlinear due to the flux-dependent current in the plasma. This nonlinearity, however, is mild and not a significant difficulty. The main issue is that plasma equilibrium is a free-boundary problem: the plasma domain  $\Omega_P$  is unknown a priori, and part of the solution.

Our problem is hence the determination of the plasma domain  $\Omega_P$  and the flux function  $\Psi$  that satisfy Equation (6.18), by means of numerical methods, such as the finite element method or more advanced discretisation techniques.

### 6.1.2 Specific problem

Based on the underlying physics, one can argue that the boundary  $\partial\Omega_P$  of the plasma (i.e., the interface between  $\Omega_P$  and  $\Omega_V$ ) is the minimal isoline of the flux function  $\Psi$ :

$$\Psi(\partial\Omega_P) = \text{constant, minimal.}$$

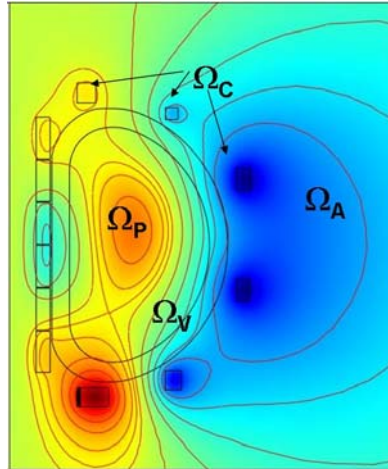


Figure 6.2: Problem domain.

Two main types of such critical isolines are possible, characterised by two different critical points; see Figure 6.3. First, a simple closed isoline tangent to the chamber wall in a limiter point (i.e., a local minimum of  $\Psi$ ). Second, a self-intersecting isoline at an  $X$ -point (i.e., a saddle point of  $\Psi$ ). The resulting equilibrium configurations are termed “limited plasma” and “diverted plasma” respectively.

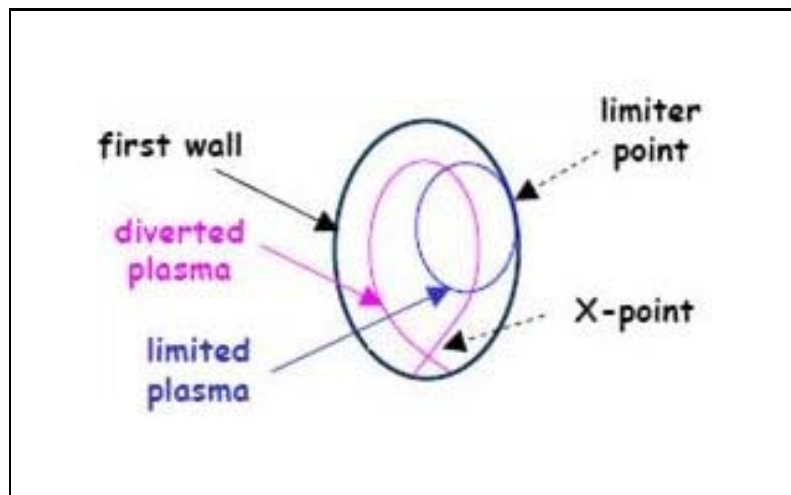


Figure 6.3: Critical isolines.

The envisaged approach is based on the iterative determination of the critical isoline: one solves the Grad–Shafranov equation with an initial guess for  $\Omega_P$ , computes the critical isoline (i.e., a new guess for  $\Omega_P$ ) as a postprocess of the solution and repeats this process up to convergence.

In this context, our specific problem can be stated as follows:

Given a finite element solution  $\Psi_H$  of the Grad–Shafranov equation, characterised by its nodal values, find the critical isoline.

In proposing an algorithm for this purpose, it is important to bear in mind that linear finite elements are the preferred option, so the Hessian matrix of the flux function  $\Psi$  is *not* readily available. Alternative procedures for the classification of critical points are required.

This report is based on contributions from the discussions held at GEMT, which included the following people: Marino Arroyo, Jordi Blasco, Josep M. Burgués, Pedro Díez, Xavier Cabré, Miquel Noguera, Marta Pellicer, Antonio Rodríguez-Ferran, Josep Sarrate, Joan Solà-Morales.

## 6.2 Classification of critical points via the index of a critical point

### 6.2.1 Motivation

In this section we propose an alternative and efficient way of facing the problem of classification of critical points of a vector field: the *index* of a *critical point*.

Essentially, we are thinking of the *winding number* of the gradient field along a closed, simple and small enough curve around the critical point. These notions can be found in Ch. V, § 36 of [1] or in Appendix II of [3], and we include them here for the self-containedness of the present report.

### 6.2.2 Informal definition

In order to get an intuition, let us first give an informal point of view of this approach. Let us consider a vector field  $\vec{V} = \vec{V}(x, y)$  on the oriented Euclidean plane. Consider also a closed curve  $\gamma$  without any singular points of the vector field on it. Choose an initial point  $P = (x_0, y_0)$  on the curve. Observe that we can associate to this point  $P$  the vector  $\vec{V}(P) = \vec{V}(x_0, y_0)$  of the vector field. If we now move the point  $P$  along the curve, the associated vector  $\vec{V}(P)$  will rotate. We can count the number of complete

rotations of this vector until  $P$  reaches its initial position again. We count the revolution as positive if  $\vec{V}(P)$  rotates in an anticlockwise direction, and negative otherwise.

So, the total number of rotations of the vector on the curve is called the *winding number of  $\vec{V}$  on  $\gamma$*  or the *index of  $\gamma$  on  $\vec{V}$* .

Several remarks can be made. The first is noticing that the index does not change under small deformations of the curve, whenever the perturbed new curve does not pass through a critical point of the field. Also, it can be seen that a curve with a non-zero index encloses—at least—one singular point of the vector field in its interior.

We now define the *index of a critical point of a vector field* as the index of a sufficiently small and closed, positively oriented curve, that encloses this point but no other singularities of the vector field in its interior. Observe that the previous remarks imply that this definition does not depend on the chosen curve, if it is small enough. For instance, we can consider a small positively oriented circumference.

Essentially, this index *counts* the number of turns that a vector field is making around the singularity. In Figure 6.4 we can see two examples for the index of a critical point. We have represented a vector field that is the gradient of a function with a maximum (at the top) and one with a saddle point (at the bottom). We want to compute the index of each point, so we choose a closed curve (in green) that encloses only this singularity for each case. In both pictures we can see the rotation of a vector of the vector field on the green curve around the singularity. An anticlockwise rotation results in index 1 for the maximum, while a clockwise rotation gives index  $-1$  for the saddle point.

If the curve (for instance the oriented boundary of a certain region) encloses several singularities, it also makes sense to compute the corresponding index. In this case, we have the following result.

**Theorem 1.** *Let us consider a domain  $\Omega$  with  $\gamma = \partial\Omega$  as the oriented curve giving the boundary. Suppose that the domain contains several singularities of the vector field in its interior (but not on the boundary). Then the index of the curve  $\gamma$  is equal to the sum of the indices of the singular points that are inside the domain  $\Omega$ .*

The index of the region will be referred to as the *global index*. We can see an example of how this index is computed in Figure 6.5. In it, we have three maxima (index  $+1$ ), two minima (index  $+1$ ) and three saddle points (index  $-1$ ). So, the global index of the domain  $\Omega$  can be computed as

$$\text{Ind}_{\Omega} = 3 \cdot (+1) + 2 \cdot (+1) + 3 \cdot (-1) = 2.$$

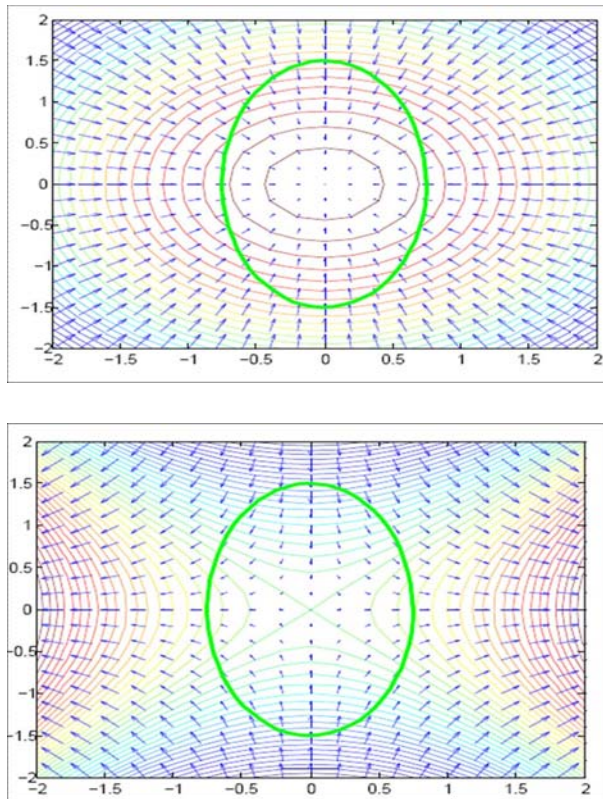


Figure 6.4: Vector field of a maximum (top) and of a saddle point (bottom).

### 6.2.3 Connection with the tokamak plasma configuration

What is the use of the index in our problem, which is to find the critical isoline of  $\Psi$  that gives the physical configuration of the plasma inside the chamber? The first thing to notice is that, for the tokamak plasma, only a few configurations are possible. Essentially, knowing the kind of critical isoline is possible in our case when we know the number of maxima and saddle points of the vector field  $\vec{V} = \nabla\Psi$  that are inside the chamber. This is possible using the global index of  $\Omega_V \cup \Omega_P$  and, if necessary, the local index of each singularity.

For instance, as we have seen in Figure 6.3 of Section 1, we have two possible plasmas: a *diverted* one (the case of a maximum and a saddle point in its interior) and a *limited* one (only a maximum in the interior). Observe that the global index allows us to distinguish between these two possible configurations, as it is 0 for the diverted plasma and +1 for the limited one.

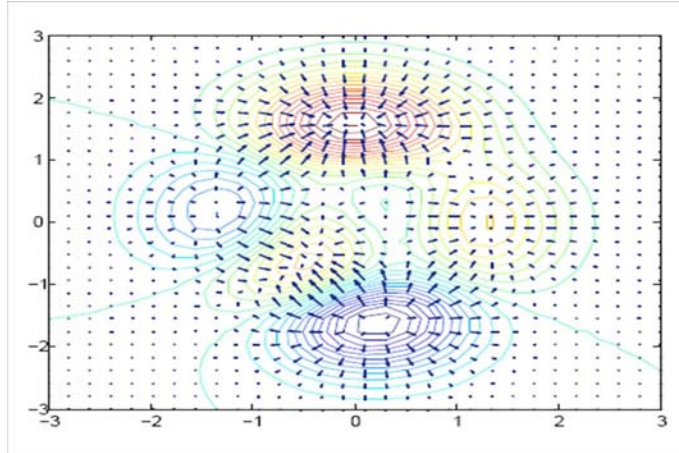


Figure 6.5: For many singularities the indices are added up. In the figure, the global index of the region is 2.

In Section 6.3 we propose an algorithm in which the index is used to distinguish between the most usual cases for the plasma configuration.

#### 6.2.4 Formal definition in a continuous setup

A rigorous definition of the index can be given (again, see [1] and [3] as references). Let us consider a vector field  $\vec{V} : \Omega \rightarrow S^1$  with norm 1, given in polar coordinates. That is,  $\vec{V}(x, y) = (r(x, y), \theta(x, y))$ , where  $r$  stands for the radius and  $\theta$  for the angle. Let us now consider a closed and oriented curve on this field,  $\gamma : S^1 \rightarrow \Omega$ .

**Definition 2.** The *index of  $\gamma$  on  $\vec{V}$*  is

$$\text{Ind}_\gamma = \frac{1}{2\pi} \oint_\gamma d\theta.$$

As  $d\theta$  is the variation of the angle and we are integrating it along the curve, it is clear that the previous definition corresponds to the informal one for the index given above. This definition allows us to rigorously prove all the *informal* results given in this section. Actually, all this relates to the so-called *topological degree theory*.

#### 6.2.5 Definition in a discrete setup

For the discrete case, the computation of the index in the case of a tokamak plasma turns out to be quite simple. As we will be using linear elements, the

gradient (that is, the vector field we are interested in) will be constant on each element. Let us call  $\vec{V}_i$  the normalized gradient vector on the  $i$ th-element, that is,

$$\vec{V}_i = \frac{\overrightarrow{(\nabla\Psi)_i}}{\|(\nabla\Psi)_i\|}.$$

Given a discrete and closed curve  $\gamma$  (for instance, the one in Figure 6.6) we can see that it passes through a finite number of elements (9 in this figure). So, we will have the corresponding  $\vec{V}_i$  for each element. Let us call  $\alpha_i$  the angle between  $\vec{V}_i$  and  $\vec{V}_{i-1}$ . Then, the (*discrete*) *index* of  $\gamma$  on the gradient vector field is:

$$\text{Ind}_\gamma = \frac{1}{2\pi} \sum_i \alpha_i.$$

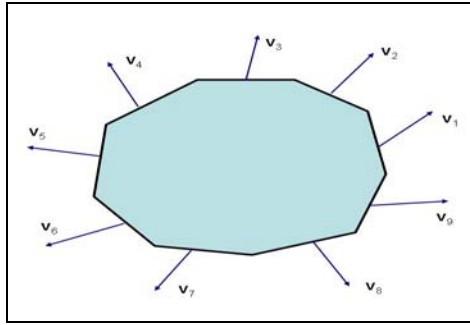


Figure 6.6: Discrete computation of the index.

The global index of a domain  $\Gamma$  is computed in the same way: we just have to consider the boundary of the domain as the curve  $\gamma$ .

### 6.3 Proposed algorithm

In this section we present the numerical algorithm proposed for the determination of the plasma region  $\Omega_P$ . The algorithm aims at determining  $\Omega_P$  from a given solution  $\Psi$  represented by a Finite Element nodal field. The overall idea of the proposed scheme consists in locating the singular points of  $\Psi$  through the vanishing of the gradient, computing the global and the local indices of  $\nabla\Psi$  and classifying the state according to the number of singular points and the values of the indices.

### 6.3.1 Computation of the gradient and gradient recovery

Step 1 consists in computing  $V = \nabla\Psi$  on every element; for linear triangular elements,  $V$  is piecewise constant. A gradient recovery technique has then to be employed to have  $V$  evaluated at the nodal points. This can be achieved by a weighted average of the elemental values on the elements to which the node belongs (weighted by the element area) or by an  $L^2$  projection onto the Finite Element space.

### 6.3.2 Singular points detection

Step 2 consists in locating the singular points of  $\Psi$ . The norm of the gradient is computed on each node, and singular points are signalled when  $\|V\| < \text{tol}\|V\|_{\max}$ , where  $\text{tol}$  is a suitable tolerance. This yields the singular points  $P_i$  for  $i = 1, \dots, N_{\text{sing}}$ .

### 6.3.3 Computation of the index

In Step 3 the global index  $\text{Ind}_{\partial\Omega_V}$  of  $\partial\Omega_V$  on  $\nabla\Psi$  is computed by the discrete algorithm described in Subsection 6.2.5 applied to the nodal representation of  $\partial\Omega_V$ , the external boundary of the vacuum region  $\Omega_V$ . The local indices  $\text{Ind}_{\partial\Omega_i}$  around each singular point  $P_i$  are computed on patches  $\Omega_i$  of elements surrounding  $P_i$ . The conservation of the property  $\text{Ind}_{\partial\Omega_V} = \sum_{i=1}^{N_{\text{sing}}} \text{Ind}_{\partial\Omega_i}$  can be a good check for this phase.

### 6.3.4 Classification of cases

In Step 4 the state of the system is classified according to the number of singular points detected and the values of the global and local indices computed. The most frequent cases are reflected in the Table 6.1. The situation in each of these cases is the following:

1. NON-EXISTENCE OF CLOSED MAGNETIC SURFACES.
2. LIMITED PLASMA. There is a tangent isoline. Its isovalue is found as the maximum of  $\Psi$  on the boundary  $\partial\Omega_V$ , which is achieved at the limiter point.
3. NON-EXISTENCE OF CLOSED MAGNETIC SURFACES. An  $X$ -point exists, but none of the two branches of its isoline lies within the chamber, and there is no other critical point in the chamber.

4. A maximum  $P_1$  and an  $X$ -point  $P_2$  exist. The isovalue of interest is the value of  $\Psi$  in  $P_2$ . Open and closed branches of the isoline can be identified by curve tracking. Two subcases are possible, which are characterized by the number of changes of the sign of  $(\Psi - \Psi(P_2))$  along the boundary  $\partial\Omega_V$ :
  - 4.1 One closed isoline inside the chamber. This is identified by two changes of sign. DIVERTED PLASMA.
  - 4.2 No closed isolines inside the chamber. This is identified by four changes of sign. NON-EXISTENCE OF CLOSED MAGNETIC SURFACES.

The remaining cases to be identified must be defined by the end-user according to his/her needs.

Case	$N_{\text{sing}}$	$\text{Ind}_{\partial\Omega_V}$	$\text{Ind}_{\partial\Omega_i}$
1	0	0	–
2	1	1	1
3	1	–1	–1
4	2	0	1, –1

Table 6.1: Classification of cases according to the number of singular points and the value of the indices.

## 6.4 Further considerations

### 6.4.1 Level set characterization of the critical isoline

In the previous sections, a methodology has been presented to compute the critical isoline from the Finite Element solution  $\Psi_H$ , characterized by its nodal values. The isoline is determined by finding the corresponding critical value of  $\Psi$ , say  $\Psi_c$ . Then, tracing the curve is a simple exercise of computational geometry. For instance, in a mesh of linear triangular elements (3-noded triangles), the iso-curve is a polygonal such that the part of it contained in every element is a straight segment. The elements crossed by the iso-curve are those such that the range of the nodal values comprises  $\Psi_c$ .

This characterization of the curve as the isoline of a contour function reminds us the well known Level Set (LS) concept [5]. An LS is an auxiliary function such that the curve to be characterized is precisely the zero iso-value. In this case, the function  $\Psi - \Psi_c$  is an LS.

An LS function  $\phi$  is defined such that its sign describes the geometrical domains using the following convention

$$\phi(\mathbf{x}, t) \begin{cases} > 0 & \text{for } \mathbf{x} \text{ in domain 1} \\ = 0 & \text{for } \mathbf{x} \text{ on the interface} \\ < 0 & \text{for } \mathbf{x} \text{ in domain 2} \end{cases} \quad (6.19)$$

where  $\mathbf{x}$  stands for a point in the simulation domain and  $t$  is the time. The interface position is the set of points where the level set field vanishes (Figure 6.7).

In common LS practice,  $\phi$  is taken as a signed distance to the interface. Far enough from the interface,  $\phi$  is truncated by maximum and minimum cutoff values. The resulting level set function describes the position of the interface independently of the computational mesh. Note that, in this case,  $\phi$  does not coincide with  $\Psi$ :  $\phi$  is only a numerical artifact describing the isoline without any precise physical meaning. The only coincidence lies in the fact that both  $\phi$  and  $\Psi - \Psi_c$  vanish at the same points.

In practical implementations,  $\phi$  is described (interpolated) with the finite element mesh, and therefore the resolution of the approximated interface depends on the quality of this mesh. Thus, the level set represents interfaces which do not necessarily coincide with the element edges. The same mesh can be used throughout the entire simulation to describe the interface.

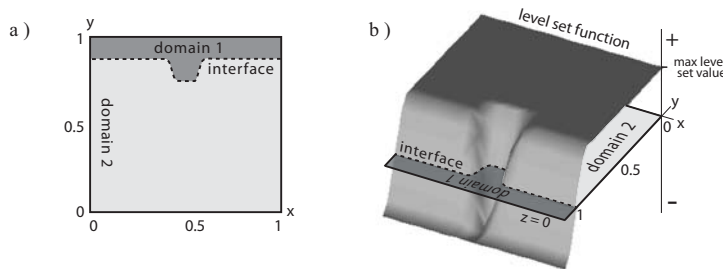


Figure 6.7: a) The two domains (materials) are associated with the sign of the level set function. The dotted line is the interface. b) Surface representation of the level set function.

Describing the curve using the LS  $\phi$  rather than  $\Psi$  is not only a matter of taste. It may bring additional advantages related to the possibility of moving the estimated boundary of  $\Omega_P$  along the iterative process in a more efficient manner.

### 6.4.2 X-FEM enrichment

The LS method is often used in combination with the so-called X-FEM (eXtended Finite Element Method); see [4, 6].

The LS approach allows the description of interphases that may cross the elements of the Finite Element mesh. Note that the phase changes are associated with discontinuities of the derivatives of the solution. Consequently, in the LS context, these discontinuities are expected to take place inside the elements. And this is something the standard finite elements cannot reproduce.

The X-FEM enriches the Finite Element discretization introducing additional interpolation functions with discontinuous derivatives across the interphase (the so-called ridge functions; see Figure 6.8 for illustration) via the Partition of the Unity Method.

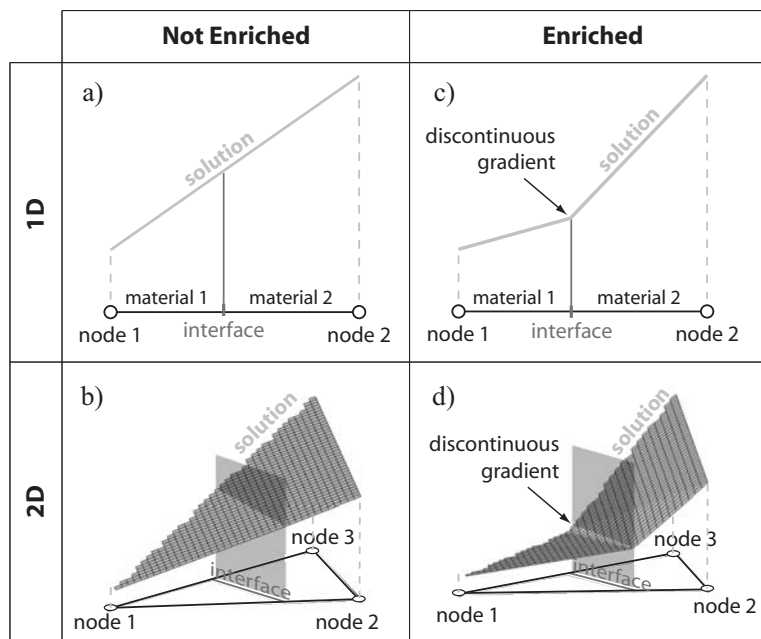


Figure 6.8: Illustration of the X-FEM enrichment both in 1D and 2D for linear elements.

Using the X-FEM would definitively increase the accuracy of the numerical approximation  $\Psi_H$  and would allow using much coarser meshes to obtain the same numerical resolution.

### 6.4.3 Analysis and possible alternative for the iterative scheme

The iterative method currently used consists in starting with an initial guess for  $\Omega_P$ , say  $\Omega_P^0$  (or, equivalently, an initial guess for  $\Psi$ , say  $\Psi_H^0$ ), then computing  $\Psi_H^1$  solving Equation (6.18) numerically. The determination of the critical isoline corresponding to  $\Psi_H^1$  yields also the new guess for  $\Omega_P$ , say  $\Omega_P^1$ , which in general does not coincide with  $\Omega_P^0$ . The same idea is used to iterate from  $\Psi_H^k$  to  $\Psi_H^{k+1}$  for  $k = 1, 2 \dots$

This iterative scheme is astonishingly simple but, according to the end-users, the observed convergence behavior is fair enough. From a mathematical viewpoint this scheme may typically show an oscillatory behavior, jumping between two solutions ( $\Psi_H^k$  leads to  $\Psi_H^{k+1}$  and  $\Psi_H^{k+1}$  leads back to  $\Psi_H^k$ ). It should be analyzed in detail in the context of the present physical problem, to understand why it is so efficient for this problem.

If a more sophisticated iterative scheme is used, based on finding the stationary/null point of some functional, it may be very useful describing the boundary of  $\Omega_P$  by an LS  $\phi$ . This would allow updating  $\Omega_P$  via  $\phi$  (from  $\phi^k$  to  $\phi^{k+1}$ ) using a standard technique as the Hamilton–Jacobi transport equation. The input for this transport equation is the advancing front velocity that has to be given by the selected iterative scheme. For instance, this velocity can be defined as a function of the difference between the critical isovalue in the consecutive iterations,  $\Psi_c^{k-1}$  and  $\Psi_c^k$ .

## Bibliography

- [1] V. I. Arnold, *Ordinary Differential Equations*, Springer Textbook, Springer-Verlag, Berlin, 1992.
- [2] P. J. Mc Carthy, *Analytical solutions to the Grad–Shafranov equation for tokamak equilibrium with dissimilar source functions*, *Physics of Plasmas* **6** (1999), 3554–3560.
- [3] S. Lefschetz, *Differential Equations: Geometric Theory*, Dover Publications, Inc., New York, 1977.
- [4] N. Moës, M. Cloirec, P. Cartraud, and J.-F. Remacle, *A computational approach to handle complex microstructure geometries*, *Computer Methods in Applied Mechanics and Engineering* **192** (2003), 3163–3177.

- [5] J. A. Sethian, *Level Set Methods and Fast Marching Methods*, Cambridge University Press, 1999.
- [6] S. Zlotnik, P. Díez, M. Fernández, and J. Vergés, *Numerical modelling of tectonic plates subduction using X-FEM*, *Computer Methods in Applied Mechanics and Engineering* **196** (2007), 4283–4293.